Langmuir Article

pubs.acs.org/Langmuir

Surface Rigidity Change of *Escherichia coli* after Filamentous Bacteriophage Infection

Yi-Yang Chen,[†] Chien-Chen Wu,[§] Jye-Lin Hsu,[‡] Hwei-Ling Peng,[§] Hwan-You Chang,[‡] and Tri-Rung Yew*,[†]

[†]*Department of Materials Science and Engineering,* [‡]*Department of Life Science, National Tsing-Hua University, 101, Section 2, Kuang-Fu Road, Hsinchu, Taiwan 30013 and* [§]*Department of Biological Science and Technology, National Chiao-Tung University, 1 Ta-Hsuie Road, Hsinchu, Taiwan 30010*

Received October 31, 2008. Revised Manuscript Received January 6, 2009

In this study, the feasibility using atomic force microscopy (AFM) to study the interaction between bacteriophages (phages) and bacteria in situ was demonstrated here. Filamentous phage M13 specifically infects the male *Escherichia coli*, which expresses F-pili. After infection, *E. coli* become fragile and grows at a slower rate. AFM provides a powerful tool for investigating these changes in a near-physiological environment. Using high-resolution AFM in phosphate-buffered saline, the damage to the lipopolysaccharide (LPS) layer on the outer membrane of the M13 phage-infected *E. coli* was observed. The membrane became smoother and more featureless compared to those that were not infected. Besides, the force−distance ($f-d$) curves were measured to reveal the surface rigidity change in *E. coli* after M13 phage infection. The effective spring constant and Young's modulus of *E. coli* decreased after M13 phage infection. Furthermore, the AFM tip was pressed against *E. coli* to study the response of *E. coli* under load before and after M13 phage infection. The results showed that after infection *E. coli* became less rigid and the membrane was also damaged. However, the stiffness changes, including the spring constant and Young's modulus of *E. coli*, are negligible after M13 phage infection compared with those in previous reports, which may be one of the reasons that *E. coli* still can maintain its viability after filamentous phage infection.

Introduction

The bacterium−bacteriophage (phage) interaction is a key concept in constructing the model in molecular biology.[1,2] In-situ observation of this interaction remains inadequate only by using optical microscopy because of its resolution limit or electron microscopy (EM) because of the sample preparation required. Recently, atomic force microscopy (AFM)[3] has emerged as a powerful tool for solving many biological issues.[4−9] The ability to image a biological sample in a near-physiological environment provides a new opportunity to study the bacterium−phage interaction with nanometer resolution. The force−distance ($f-d$) curve obtained by AFM can also provide information about the molecular interactions and mechanical properties (e.g., spring constant and Young's modulus) of samples.[8,10−14] The AFM images in liquid combined with $f-d$ curves enable research on the single-cell or even single-molecule level.[15,16] AFM, therefore, was used to study the interaction between filamentous phage M13 and *Escherichia coli*.

Filamentous phage M13, which is about 6 to 7 nm in diameter and 1 μm in length, specifically infects male *E. coli*, which expresses F-pili. The F-pili can serve as a receptor for phage infection.[17−19] The infection process of a filamentous phage consists of three steps: attachment, penetration, and secretion.[19,20] The filamentous phage first attaches to the tip of the F-pilus, and the DNA of the phages penetrates the *E. coli* cell through the F-pilus channel or by the retraction of the F-pilus. During the stage of secretion, the replicated phage will assemble at the cell membrane and will be extruded by *E. coli*.[17−19,21−25]

*Corresponding author. E-mail: tryew@mx.nthu.edu.tw. Tel: +886-936347230. Fax: +886-3-5722366.

(1) Dubrovin, E. V.; Voloshin, A. G.; Kraevsky, S. V.; Ignatyuk, T. E.; Abramchuk, S. S.; Yaminsky, I. V.; Ignatov, S. G. *Langmuir* **2008**, *24*, 13068–13074.
(2) Kay, L. E. *J. Hist. Biol.* **1985**, *18*, 207–246.
(3) Binnig, G.; Quate, C. F.; Gerber, C. *Phys. Rev. Lett.* **1986**, *56*, 930–933.
(4) Drygin, Y. F.; Bordunova, O. A.; Gallyamov, M. O.; Yaminsky, I. V. *FEBS Lett.* **1998**, *425*, 217–221.
(5) Dufrene, Y. F. *Curr. Opin. Microbiol.* **2003**, *6*, 317–323.
(6) Fotiadis, D.; Scheuring, S.; Muller, S. A.; Engel, A.; Muller, D. J. *Micron* **2002**, *33*, 385–397.
(7) Gad, M.; Ikai, A. *Biophys. J.* **1995**, *69*, 2226–2233.
(8) Kuznetsova, T. G.; Starodubtseva, M. N.; Yegorenkov, N. I.; Chizhik, S. A.; Zhdanov, R. I. *Micron* **2007**, *38*, 824–833.
(9) Ohnesorge, F. M.; Horber, J. K. H.; Haberle, W.; Czerny, C. P.; Smith, D. P. E.; Binnig, G. *Biophys. J.* **1997**, *73*, 2183–2194.
(10) Arnoldi, M.; Fritz, M.; Bauerlein, E.; Radmacher, M.; Sackmann, E.; Boulbitch, A. *Phys. Rev. E* **2000**, *62*, 1034–1044.
(11) Dupres, V.; Menozzi, F. D.; Locht, C.; Clare, B. H.; Abbott, N. L.; Cuenot, S.; Bompard, C.; Raze, D.; Dufrene, Y. F. *Nat. Methods* **2005**, *2*, 515–520.
(12) Sullivan, C. J.; Morrell, J. L.; Allison, D. P.; Doktycz, M. J. *Ultramicroscopy* **2005**, *105*, 96–102.
(13) Sullivan, C. J.; Venkataraman, S.; Retterer, S. T.; Allison, D. P.; Doktycz, M. J. *Ultramicroscopy* **2007**, *107*, 934–942.
(14) Velegol, S. B.; Logan, B. E. *Langmuir* **2002**, *18*, 5256–5262.
(15) Chtcheglova, L. A.; Shubeita, G. T.; Sekatskii, S. K.; Dietler, G. *Biophys. J.* **2004**, *86*, 1177–1184.
(16) Seong, G. H.; Niimi, T.; Yanagida, Y.; Kobatake, E.; Aizawa, M. *Anal. Chem.* **2000**, *72*, 1288–1293.
(17) Caro, L. G.; Schnos, M. *Proc. Natl. Acad. Sci. U.S.A.* **1966**, *56* 126–132.
(18) Jacobson, A. *J. Virol.* **1972**, *10*, 835–843.
(19) Novotny, C.; Raizen, E.; Knight, W. S.; Brinton, C. C., Jr. *J. Bacteriol.* **1969**, *98*, 1307–1319.
(20) Roy, A.; Mitra, S. *J. Virol.* **1970**, *6*, 333–339.
(21) Bradley, D. E.; Dewar, C. A. *J. Gen. Virol.* **1967**, *1*, 179–188.
(22) Brinton, C. C., Jr.; Gemski, P., Jr.; Carnahan, J. *Proc. Natl. Acad. Sci. U.S.A.* **1964**, *52*, 776–783.
(23) Novotny, C.; Knight, W. S.; Brinton, C. C.Jr. *J. Bacteriol.* **1968**, *95*, 314–326.
(24) Shu, A. C.; Wu, C. C.; Chen, Y. Y.; Peng, H. L.; Chang, H. Y.; Yew, T. R. *Langmuir* **2008**, *24*, 6796–6802.
(25) Valentine, R. C.; Strand, M. *Science* **1965**, *148*, 511–513.

In the secretion step of the phage infection process, the filamentous phages do not lyse the *E. coli*.[20,26] However, the infected *E. coli* becomes fragile and grows at a slower rate compared to those that are not infected.[20] Some electron microscopy studies have suggested that during the process of phage secretion the holes generated by phage proteins in the cellular membrane may cause cytoplasm leaking, which may lead cells to become empty.[21] Nevertheless, there has been evidence showing that the lipopolysaccharide (LPS), which serves as a permeability barrier at the outer bacterial membrane to protect bacteria and is believed to contribute the structural rigidity of the cell envelope,[27,28] is damaged and released.[20]

In this study, the nanomechanical properties of *E. coli* before and after filamentous phage M13 infection were investigated by AFM. The high-resolution images of the *E. coli* membrane and *f*−*d* curves on *E. coli* were used to investigate the impact of the M13 phage on the bacteria in phosphate-buffered saline (PBS). Also, the AFM tip was pressed against the bacteria to study the response of *E. coli* under load. As a comparison, ethylenediamine teraacetate (EDTA)[29] was used to treat the bacteria to demonstrate how the releasing of LPS from the *E. coli* outer membrane affects the nanomechanical properties of *E. coli*. This study demonstrates the feasibility of using AFM as a powerful tool to investigate the bacterium−phage interaction in situ. In particular, the nanomechanical properties can be fully studied by using the *f*−*d* curves.

Materials and Methods

Bacterial Culture Condition, Harvesting, and M13 Phage Infection. *E. coli* strain JM109 (ATCC 53323 e14$^-$(McrA$^-$) *recA1 endA1 gyrA96 thi-1 hsdR17* (*r*K$^-$*m*K$^+$) *supE44 relA1* Δ(*lac-proAB*) [F′ *traD36 proAB lacI*q*Z*Δ*M15*]) (Biosource Collection and Research Center, Hsin-chu, Taiwan) was used in this study and propagated in Luria−Bertani (LB) broth (MDBio Inc., Taipei, Taiwan) at 37 °C. *E. coli* cells cultured overnight were co-incubated with or without M13 phage (M13mp18) (Biosource Collection and Research Center, Hsin-chu, Taiwan) and refreshed to the midexponential phase. The *E. coli* was then harvested at the midexponential phase and washed three times with PBS.

Filamentous Phage Infection Confirmation. The immunofluorescence assay was used to examine the infection percentage of *E. coli* by the M13 phage in this work. *E. coli* with and without M13 phage infection was first immobilized on a glass slide by heating to 60 °C. The *E. coli* was then incubated with anti-M13 polyclonal antibody (Amersham Biosciences, Arlington Heights, IL) for 2 h and anti-FITC antibody (Amersham Biosciences, Arlington Heights, IL) for another 2 h. After being rinsed with deionized water, the samples were observed via fluorescence microscopy (Olympus BX-51 equipped with Diagnostic Spot RT-SE digital CCD camera).

Release the LPS Layer from the Bacteria Membrane. The *E. coli* harvested in the midexponential phase were incubated in 100 mM EDTA/PBS at 37 °C for 40 min.[30] The bacteria were then washed two times with PBS and resuspended in PBS for analysis.

Hydrophobicity of a Bacterium Surface. The hydrophobicity of the bacteria membrane is measured via the water contact angle[31,32] on a homemade instrument that includes an optical microscope (400×) equipped with charge-coupled devices (ChipER Tech., Panchiao, Taiwan). A solution with 3 mL of the cell suspensions prepared as described above was filtered through a 0.45 μm filter (Amersham Biosciences, Arlington Heights, IL). After 45 min of air drying in a relatively humid environment (73−76% RH), to prevent full dehydration and the best drying time as reported for the bacteria lawn,[27] approximate 10 μL of deionized water was dropped onto the bacteria lawn. The image was then recorded with a CCD camera for contact angle analysis.

Sample Preparation for AFM Observation. *E. coli* images were scanned by AFM in both air and liquid. An important issue in observing bacteria in liquid by AFM is to immobilize the bacteria on a supporting substrate such as mica or a cover glass slide. Because the strong lateral force during AFM raster scanning may cause the bacteria to detach from the substrate surface and move along with the AFM tip, various methods of substrate surface modification to immobilize bacteria have been proposed for AFM imaging.[12,33,34] With a successful substrate surface modification and immobilization process, the bacterial membrane can be clearly imaged, which is attributed to the *E. coli* cells' adherence to the substrate surface after immobilization. However, the surface modification could lead to an increase in substrate surface roughness and difficulties in imaging and identifying the filamentous structure around *E. coli*.

E. coli imaging in air was conducted to assist the analysis of bacterium−phage interaction. For the preparation of the dry sample imaged in air, the bacteria suspension was washed with deionized water and diluted 100-fold with deionized water to achieve a concentration of approximate 10^3 cells/mL. Following that, 100 μL of the bacteria suspension in deionized water was dropped onto newly cleaved mica and a cover glass slide and fully dehydrated in air by heating the sample to 60 °C for AFM observation. As for the sample-preparation process for AFM imaging in liquid, poly-L-lysine (PLL)-coated mica was used for bacteria immobilization. PLL mica was prepared by drying 100 μL of a 0.01 wt % PLL solution (P8920, Sigma-Aldrich, St. Louis, MO) on newly cleaved mica overnight.[33] The PLL mica was then rinsed three times with PBS before being used. The 100 μL of a bacteria suspension in PBS with approximate 10^5 cells/mL was applied to the PLL mica. The excess liquid was then drained after 10 min to allow the bacteria to adhere. Another 10 min of air drying was then conducted before AFM observation, which is believed not to harm the bacteria but is crucial for *E. coli* immobilization.[33] The 200 μL fresh, cold PBS solution was refilled for the mica, and the sample was ready for AFM observation.

AFM Imaging and Force−Distance and Force−Time Curve Acquisition. AFM measurements in liquid were conducted by using Nanowizard I (JPK Instrument, AG Berlin, Germany) at room temperature. The *z* position of the piezo of the AFM was calibrated with a strain gauge, and the *x* and *y* positions were calibrated with capacitance values. Bacteria images in air were obtained in contact mode using a commercial Si AFM tip (CSC-38) with a spring constant of 0.03 N/m (Mikromasch, Tallinn, Estonia), provided by Dimension 3100 (Veeco, Santa Barbara, CA).

For in-situ observation of the bacteria, each experiment lasted no longer than 2 h to prevent any potential bacteria change due to environmental changes such as the temperature

(26) Stopar, D.; Spruijt, R. B.; Wolfs, C. J.; Hemminga, M. A. *Biochim. Biophys. Acta* **2003**, *1611*, 5–15.
(27) Atabek, A.; Camesano, T. A. *J. Bacteriol.* **2007**, *189*, 8503–8509.
(28) Salton, M. R. *Annu. Rev. Microbiol.* **1967**, *21*, 417–442.
(29) Voll, M. J.; Leive, L. *J. Biol. Chem.* **1970**, *245*, 1108–1114.
(30) Amro, N. A.; Kotra, L. P.; Wadu-Mesthrige, K.; Bulychev, A.; Mobashery, S.; Liu, G. Y. *Langmuir* **2000**, *16*, 2789–2796.
(31) Burks, G. A.; Velegol, S. B.; Paramonova, E.; Lindenmuth, B. E.; Feick, J. D.; Logan, B. E. *Langmuir* **2003**, *19*, 2366–2371.
(32) Ong, Y. L.; Razatos, A.; Georgiou, G.; Sharma, M. M. *Langmuir* **1999**, *15*, 2719–2725.
(33) Bolshakova, A. V.; Kiselyova, O. I.; Filonov, A. S.; Frolova, O. Y.; Lyubchenko, Y. L.; Yaminsky, I. V. *Ultramicroscopy* **2001**, *86*, 121–128.
(34) Doktycz, M. J.; Sullivan, C. J.; Hoyt, P. R.; Pelletier, D. A.; Wu, S.; Allison, D. P. *Ultramicroscopy* **2003**, *97*, 209–216.

and lack of nutrition. A pyramid-shaped Si_3N_4 AFM tip (PNP-DB, Nanoworld, Neuchatel, Switzerland) with a spring constant of 0.2 N/m determined by the thermonoise method[35] was used for AFM imaging in liquid, $f-d$ curves, and force−time measurements. AFM images were processed with JPK SPM image processing v.3 software. Bacteria images were first obtained by scanning with tapping mode. After the position of the bacterium was located, the AFM operation mode was switched to contact mode for $f-d$ curves. Three random locations on the same bacteria, usually two polar points and a middle point of the cell, were selected to record the $f-d$ curves. Each point was performed five times to get an average value. The force applied to *E. coli* was 3 nN, which will not cause harm to the *E. coli* because identical $f-d$ curves can be obtained on the same location.

As for the force−time curves, a schematic for obtaining the force−time relationship is shown in Figure 1. The AFM tip was first brought into contact with the bacterium surface as shown in A and B. After the AFM tip touched the surface, the AFM tip was then pressed against the bacterium until the force reached the set point (3 nN, cantilever deflection × spring constant of AFM tip = 15 nm × 0.2 N/m) as shown in B and C. After the force reached 3 nN, the AFM cantilever base was kept at a constant height as shown in C and D in Figure 1. The cantilever deflection versus time was then recorded to obtain a force−time curve. Finally, the tip was detached from the bacterium and return to its original point as shown in D−F after the force−time curve was recorded. In this work, one to two random locations on each bacterium were selected, and only the first force−time curve was used for analysis.

Evaluation of the Effective Spring Constant and Young's Modulus. A simple model assuming the AFM cantilever and bacterium to be two ideal springs in series proposed by Arnoldi[10] was used to calculate the effective spring constant

$$k_c = \frac{k_a \times m}{1 - m} \quad (1)$$

where k_c is the effective spring constant of the bacterium cell, k_a is the spring constant of the AFM tip, and m is the slope of the linear part for the extended $f-d$ curves.

The Young's modulus was calculated using the Hertz model proposed by Gaboriaud,[36] shown below

$$F = \frac{2}{\pi}\frac{E}{(1-\gamma^2)}\tan(\alpha)\delta^2 \quad (2)$$

where α is the half-cone angle and is set to 35°, γ is the Poisson ratio and is assumed to be 0.5 for soft materials, E is the Young's modulus, δ is the indentation depth of the AFM tip, and F is the force that the AFM tip applied to a bacterium. The nonlinear part of the extended $f-d$ curve was fitted with eq 2 to calculate the Young's modulus.

Results and Discussion

Infection Percentage of Bacteria by the M13 Phage. The percentage of *E. coli* infected with the M13 phage was examined by immunofluorescence assay, and almost 99% of cells were infected with the M13 phage. Figure 2a,b shows the optical and fluorescence images of *E. coli* cells, and Figure 2c,d shows those of *E. coli* cells infected with the M13 phage. In Figure 2b, no green fluorescence was observed, indicating that no M13 phages exist, whereas the green fluorescence in Figure 2d confirms that the M13 phages were secreted by the bacteria. The nanomechanical properties of *E. coli* that were secreting M13 phages were studied and compared with noninfected *E. coli*.

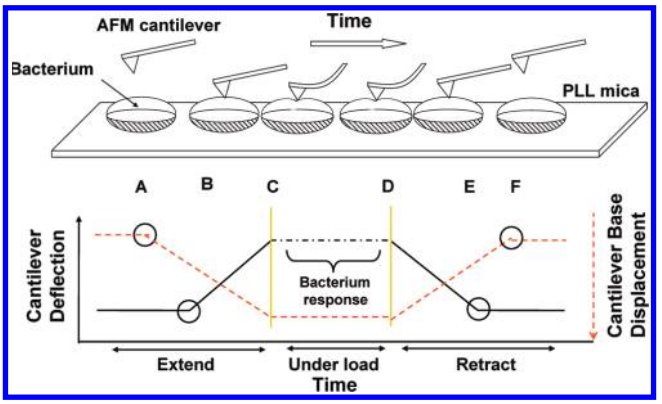

Figure 1. Schematic diagram of the relative position of the AFM cantilever base and its correlation with the AFM cantilever deflection versus time (force−time curve). The AFM tip was first brought into contact with a bacterium (A and B). After the tip touched the bacterium surface, the AFM tip continued to indent until the force reached the set point (3 nN) (B and C). The AFM cantilever base was kept at a constant height, and the force−time curve was recorded to study the interaction between the AFM tip and bacterium. After the force−time curve was recorded, the AFM tip was detached and reverted back to its original position (D−F).

Hydrophobicity of the Bacterium Surface. Table 1 shows the contact angle measurement of the filter without *E. coli*, *E. coli* before infection, *E. coli* infected with the M13 phage, and *E. coli* treated with EDTA. The filter without *E. coli* is relatively more hydrophobic (40 ± 3°) than that with the bacteria lawn. After M13 phage infection and EDTA treatment, the bacteria lawn becomes more hydrophobic, with the contact angles of water increasing from 17 ± 2° to 33 ± 5° and 31 ± 3° for M13-infected and EDTA-treated *E. coli*, respectively. The coat protein of the M13 phage exposed outside is usually considered to be hydrophilic. Therefore, the contribution of the M13 phage to the hydrophobicity could be ignored because the measured bacterium surface was more hydrophobic after M13 phage infection. These results are similar to the observation reported by Burks and Ong.[31,32] They observed that *E. coli* with a mutant has a different LPS length and found that the hydrophobicity of the bacteria changed with different LPS length. By comparing the macroscopic measurements, a change in the outer membrane was observed and was possibly due to the damage of the LPS.

AFM Images of Bacteria. A typical AFM height image, a lateral force image, and a cursor plot for the filamentous structure of *E. coli* in air without M13 phage infection are shown in Figure 3a−c, respectively, whereas those for *E. coli* infected with the M13 phage are shown in Figure 3d−f, respectively. Figure 3g shows the AFM image of the M13 phage obtained from the supernatant from the bacteria culture solution after centrifugation, and Figure 3h shows its cursor plot. There are many filamentous structures observed around the *E. coli* and M13-infected *E. coli* in Figure 3a,b and Figure 3d,e. The filamentous structures around noninfected *E. coli* are less than 5 nm in height as shown in Figure 3c, and those around M13-infected *E. coli* are about 6 to 7 nm, as shown in Figure 3f. Therefore, the filamentous structures for *E. coli* without M13 phage

(35) Hutter, J. L.; Bechhoefer, J. *Rev. Sci. Instrum.* **1993**, *64*, 1868–1873.
(36) Gaboriaud, F.; Dague, E.; Bailet, S.; Jorand, F.; Duval, J.; Thomas, F. *Colloids Surf., B* **2006**, *52*, 108–116.

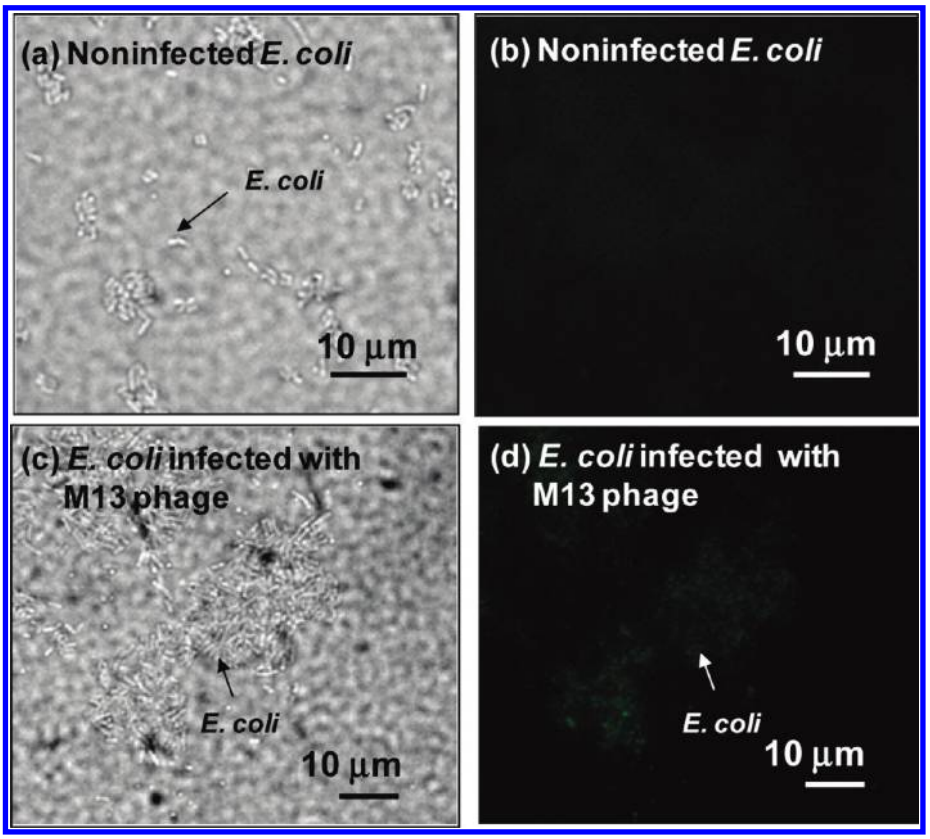

Figure 2. (a) Optical and (b) fluorescence images of noninfected *E. coli* and (c) optical and (d) fluorescence images of *E. coli* infected with the M13 phage. The green fluorescence in image (d) indicates the existence of the M13 phage. No green fluorescence can be observed because only *E. coli* cells are present in image (b). The bacteria exhibit green fluorescence in image (d), indicating that the bacteria have been infected with the M13 phage ($n = 3$ experiments).

Table 1. Water Contact Angle on the Bacteria Lawn

	filter without *E.coli*	noninfected *E. coli*	*E. coli* infected with M13 phage	*E. coli* treated with EDTA
water contact angle	40 ± 3°	17 ± 2°	33 ± 5°	31 ± 3°
experiment	3	3	3	3

infection are considered to be pili, whereas those for *E. coli* with M13 phage infection are regarded as M13 phagelike by comparing their height with that of the M13 phage in Figure 3g. The cursor plot was used instead of directly measuring the vertical distance of the height image in order to avoid the tip deconvolution effect. The loss of LPS could cause changes in the dynamic structure of outer membranes. Consequently, the expression and distribution of the usher proteins, which are the anchor for the assembly of pili onto the outer membrane, may also be influenced. This may be the reason that pili cannot be observed after M13 phage infection in Figure 3d,e. Nevertheless, the M13 phages were identified by the immunofluorescence assay instead of the AFM images shown here.

The dehydration process in preparing the sample in air will cause an artifact in the bacteria. When dealing with the mechanical properties of the bacteria, keeping the observation in PBS should be a better choice. Figure 4a−c shows the AFM 3D height images in PBS for noninfected *E. coli*, for *E. coli* with M13 phage infection, and for *E. coli* with 100 mM EDTA treatment, respectively. The height images were mapped with phase images to enhance the contrast further. The membranes of *E. coli* were enlarged to observe the difference in the membranes after M13 phage infection and EDTA treatment. Figure 4d−f shows the membrane of *E. coli*, *E. coli* infected with M13 phage, and *E. coli* treated with EDTA, respectively. Because of the PLL coated on the mica, the phages around the M13-infected *E. coli* cannot be clearly imaged by AFM in liquid. No significant changes were observed in shape and size between *E. coli* before infection and M13-infected *E. coli*. The rod shape is maintained in most of the bacteria before and after M13 phage infection, which can be observed in Figure 4a,b, respectively. The cell height, however, significantly decreases, usually by more than 100 nm, after 100 mM EDTA treatment. The reasons that EDTA will cause the cell height to decrease is still unclear.[30] In general, EDTA will release the LPS from the bacterial membrane.

Comparing Figure 4d−f clearly shows that after M13 phage infection and EDTA treatment the outer membrane of *E. coli* becomes smooth and featureless compared with those that are noninfected. The bumps on the *E. coli* outer membrane in Figure 4d were believed to be the LPS bundles[30] that disappeared after M13 phage infection and EDTA treatment, as shown in Figure 4e,f, respectively. The small features on the membrane of Figure 4e,f were not taken into account mainly because they were too small (about 5 nm × 5 nm) compared to the tip size (10−15 nm). Consequently, the rms roughness value of the membrane was calculated to show the difference. Table 2 shows the rms roughness of *E. coli* before and after M13 phage infection and EDTA treatment. It reveals that the rms roughness decreases from 5.62 ± 1.28 to 3.67 ± 1.26 and 3.98 ± 1.00 nm after M13 phage infection and EDTA

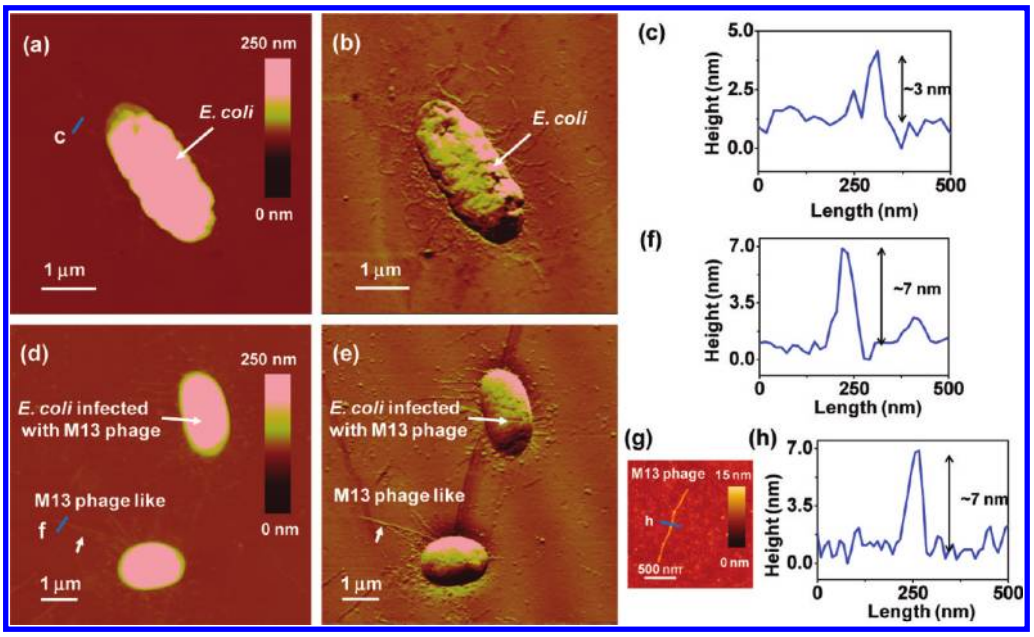

Figure 3. Typical AFM height image, lateral force image, and cursor plot for the filamentous structure of *E. coli* in air without M13 phage infection are shown in (a)−(c), respectively, and those for *E. coli* with M13 phage infection are shown in (d)−(f), respectively. (g) AFM image of the M13 phage obtained from the supernatant of the bacteria culture solution after centrifugation. (h) Cursor plot of its filamentous structure. (c) Cursor plot of the filamentous structure in image (a), which is regarded as pili by its height (less than 5 nm). (f) Cursor plot of the filamentous structure in (d), which is considered to be M13 phagelike by its height (about 6 to 7 nm). The blue lines in (a), (d), and (g) are the traces of AFM tip scans for cursor plots.

treatment, respectively. Comparing the results, the disappearance of the bumps and the decrease in the rms roughness mainly resulted from the damage to the LPS on the outer *E. coli* membrane due to the M13 phage infection.

Effective Spring Constant and Young's Modulus. After M13 phage infection, the outer membrane of the *E. coli* was damaged. The $f-d$ curves were used to reveal the rigidity change due to the damaged LPS. Typical $f-d$ curves of mica, *E. coli* before infection, *E. coli* infected with M13 phages, and *E. coli* treated with EDTA are shown in Figure 5. The effective spring constant can be calculated by the linear part of the $f-d$ curve and is related to the turgor pressure of the bacteria.[10] The effective spring constant decreases from 0.0368 ± 0.01 to 0.0180 ± 0.0034 N/m after M13 phage infection and to 0.0182 ± 0.0039 N/m after EDTA treatment, as shown in Figure 6a−c, respectively.

The damage and release of the LPS from the *E. coli* at the outer membrane is suspected to be the cause that leads to the decreases in the effective spring constant, though a few reasons may be considered. The change in the bacteria turgor pressure due to different osmotic pressure[13] could be excluded because all experiments were performed in PBS at a constant pH value throughout the whole experiment. Another possibility is that the difference might come from the change "inside" of the bacteria, such as the leakage of the cytoplasm proposed by Bradley,[21] because the release of the dense material cytoplasm may cause the turgor pressure of a bacterium to decrease. However, no significant change in the dimensions of *E. coli* after M13 phage infection has been observed, which implies that there should be no leakage of the cytoplasm. Therefore, the decrease in the spring constant is mostly due to the damage and release of the LPS layer. EDTA was reported to extract divalent metal ions such as Ca^{2+} and Mg^{2+}, weaken the LPS interaction, and cause the release of LPS from the outer membrane of *E. coli*.[20,30,37−39] As reported by Amro,[30] the percentage of LPS remaining on the bacterial surface is about 40% after 100 mM EDTA treatment. A very similar result between M13-phage-infected and 100 mM EDTA-treated *E. coli* was obtained here. Hence, the decrease in the spring constant is most likely caused by damage to the membrane, in which the LPS layer was damaged and released as proposed by Roy.[20]

As for the nonlinear part of the $f-d$ curves, the Hertz model was used to calculate the Young's modulus. The nonlinear part of the $f-d$ curve was mostly due to the cell elasticity change during the indentation.[14] Figure 6d−f shows the Young's moduli of noninfected *E. coli*, *E. coli* after M13 phage infection, and *E. coli* with EDTA treatment, respectively. The Young's moduli decrease from 0.365 ± 0.122 Mpa for *E. coli* without M13 phage infection to 0.158 ± 0.068 Mpa for *E. coli* infected with M13 phage to 0.101 ± 0.056 Mpa for *E. coli* treated with EDTA. The nonlinear part of the $f-d$ curves increased from about 50 to 100 nm after M13 phage infection and EDTA treatment. The decrease in the Young's modulus and increase in the nonlinear part of the $f-d$ curves indicate further damage, which is possible in the peptidoglycan layer of the outer membrane resulting from M13 phage infection.

As proposed by Velegol in 2002[14] and Francius in 2008,[40] the nonlinear deformation of the $f-d$ curve will dominate until the AFM tip contacts the peptidoglycan layer, which maintains the cellular architecture, and then the $f-d$ curve will become linear. Therefore, the increase in the nonlinear part and the decrease in the Young's modulus imply damage to the outer membrane, such as the peptidoglycan layer.

(37) Bayer, M. E.; Leive, L. *J. Bacteriol.* **1977**, *130*, 1364–1381.
(38) Leive, L. *Biochem. Biophys. Res. Commun.* **1965**, *21*, 290–296.
(39) Leive, L. *Ann. N.Y. Acad. Sci.* **1974**, *235*, 109–129.
(40) Francius, G.; Domench, O.; Mingeot-Leclercq, M. P.; Dufrene, Y. F. *J. Bacteriol.* **2008**, *190*, 7904–7909.

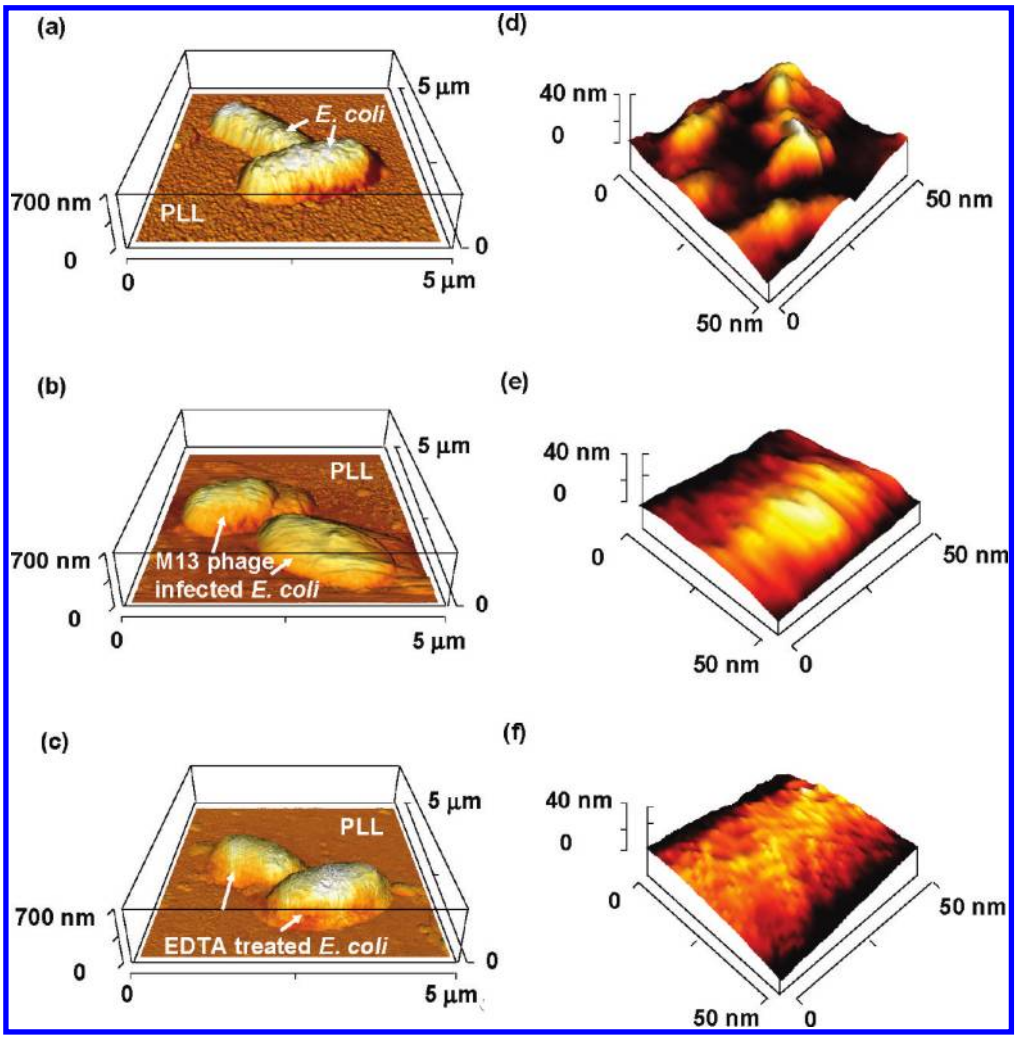

Figure 4. AFM images of bacteria in PBS for (a) noninfected *E. coli*, (b) *E. coli* infected with M13 phages, and (c) *E. coli* treated with 100 mM EDTA and their respective high-resolution AFM images of membranes in (d)−(f), respectively. The AFM images in (a), (b), and (c) show no significant difference except that the cell height decreases after EDTA treatment. However, the membrane surfaces of the *E. coli* in (d)−(f) are different. The bumps on the cell membrane of the noninfected *E. coli* in image (a) are believed to be the LPS bundles. After infection and EDTA treatment, the bumps disappear in image (e) and (f), which is evidence that the LPS layer has been damaged.

Table 2. rms Roughness of the Bacteria Membrane

	noninfected *E. coli*	*E. coli* infected with M13 phage	*E. coli* treated with EDTA
rms roughness (nm)	5.62 ± 1.28	3.67 ± 1.26	3.98 ± 1.00
bacterium	10	8	7

Though the effective spring constant and Young's modulus show that after M13 phage infection the bacterium does become weaker, the stiffness changes between noninfected *E. coli* and that infected with M13 phages are relatively small. As reported by Gaboriaud in 2006, the stiffness of the bacteria changes from 0.037 Mpa at pH 10 to 0.21 Mpa at pH 4,[41] which is much larger than we report here. The negligible change measured in this work may be related to the fact that the filamentous phage does not disturb the host bacteria and the viability of the bacteria is still maintained.[26] In general, the spring constant and Young's modulus show that after M13 phage infection *E. coli* became softer because of the damage to membrane such as the LPS and peptidoglycan layer. Besides, there are no significant changes in the height of *E. coli* after M13 phage infection, showing that the leakage of cytoplasm is unlikely and the bacteria remained intact.

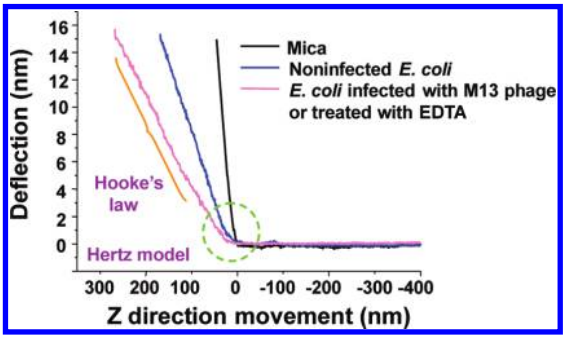

Figure 5. Typical force−distance curves of mica, noninfected *E. coli*, *E. coli* infected with M13 phages and *E. coli* treated with EDTA. The slope shows the hardness of the measured surface. Hooke's theory was used to calculate the effective spring constant by using the slope of the linear part in the extended curves. The nonlinear part was used to extract the Young's modulus by applying the Hertz model.

Response of Bacteria under Load. The AFM tip was pressed against the bacterium at 3 nN to study the

(41) Gaboriaud, F.; Bailet, S.; Dague, E.; Jorand, F. *J. Bacteriol.* **2005**, *187*, 3864–3868.

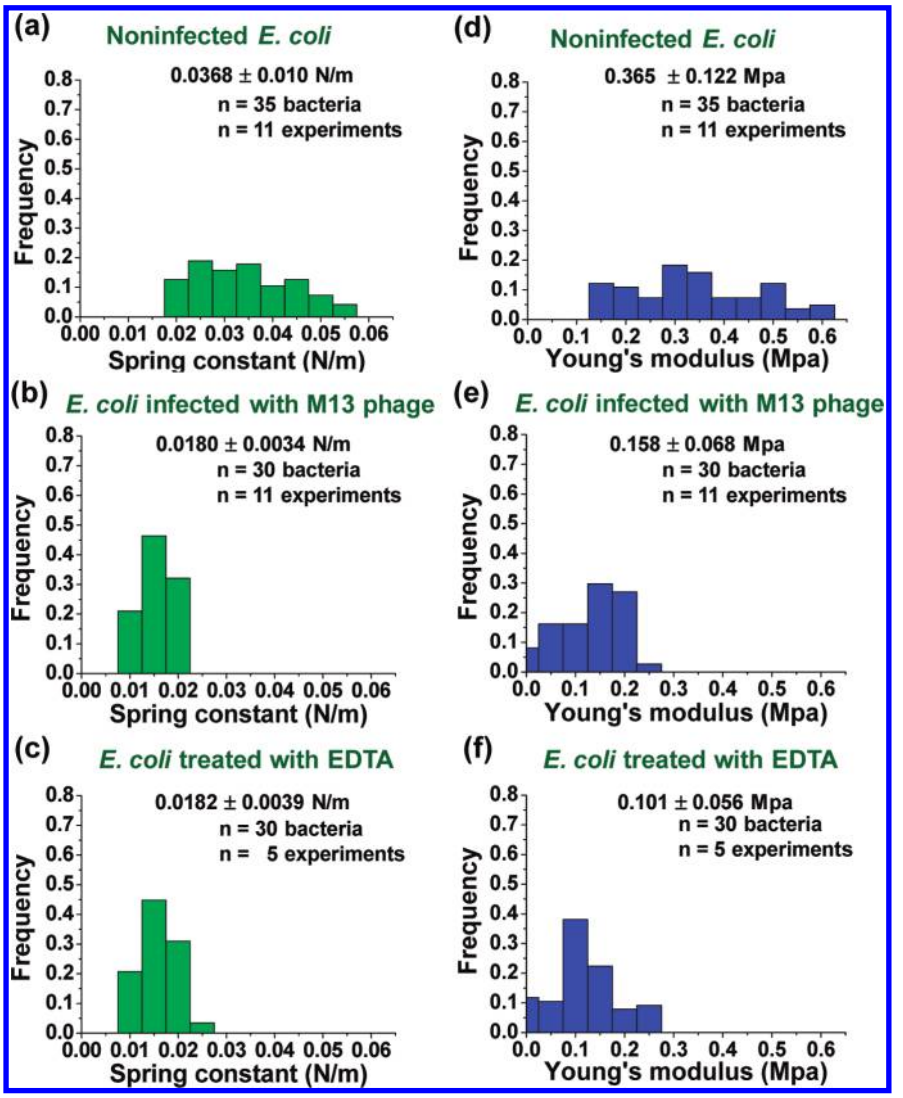

Figure 6. Distribution of the effective spring constant and Young's modulus for (a) noninfected *E. coli*, (b) *E. coli* infected with M13 phages, and (c) *E. coli* treated with 100 mM EDTA and their respective Young's moduli in (d)−(f).

response of bacteria under load, as shown in Figure 7a,b for the response of noninfected *E. coli* and that infected with M13 phages, respectively. Their differences between the contact point and detachment point (Δn) shown in Figure 7c,d, respectively, exhibit different behaviors. *E. coli* without M13 phage infection exhibits a positive Δn value indicating that the AFM tip has experienced a repulsive force. As for *E. coli* infected with M13 phages, a negative Δn can be observed, and the deflection decreases exponentially.

The positive Δn shown in Figure 7c indicates that a repulsive force appears when the tip and bacterium surface are brought into contact with each other. An outer-membrane polymer such as LPS can serve as a steric barrier to protect bacteria and cause a repulsive force. The behavior of M13-infected *E. coli* under load shows that the stress applied by the tip is released exponentially, which is similar to that observed by Vadillo-Rodriguez[42] and Okajima.[43] The observed stress relaxation behavior of the bacterium cell proved that the cell was stiff enough to maintain the shape of the bacterium and ductile enough to allow expansion.[14] Nevertheless, the reasons causing the difference in stress relaxation behavior and between noninfected bacteria and M13-infected bacteria still remain unclear and need further study.

In summary, the surface rigidity change in the bacteria after filamentous phage M13 infection has been demonstrated here. The effective spring constant and Young's modulus decrease after M13 phage infection and EDTA treatment were mostly caused by the release of LPS from the damage of the outer membrane. The change in the bacterium surface morphology due to the release of LPS was also observed by AFM imaging. Furthermore, the response of bacteria under load was studied by pressing the bacteria with a force of 3 nN, showing the different behavior and surface properties between *E. coli* before and after M13 phage infection, though their difference in rigidity changes and the dimensions are negligible. Also, the M13-infected *E. coli* still exhibits the ability to release stress.

On the basis of the above results, the feasibility of using AFM as a tool for observing the bacterium−phage interaction was demonstrated here. The studies in

(42) Vadillo-Rodriguez, V.; Beveridge, T. J.; Dutcher, J. R. *J. Bacteriol.* **2008**, *190*, 4225–4232.
(43) Okajima, T.; Tanaka, M.; Tsukiyama, S.; Kadowaki, T.; Yamamoto, S.; Shimomura, M.; Tokumoto, H. *Nanotechnology* **2007**, *18*, 084010.

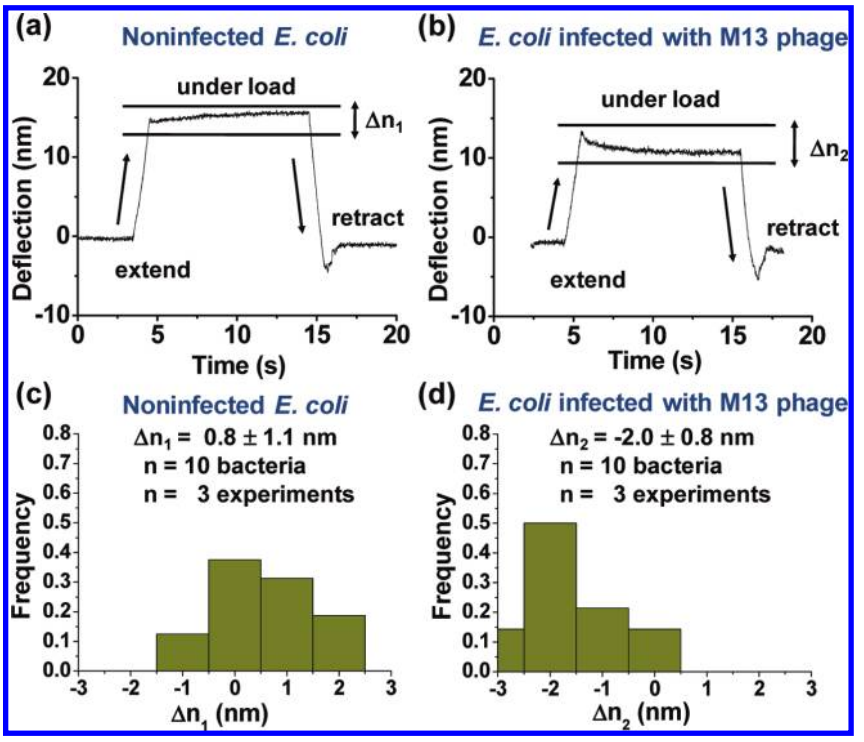

Figure 7. Typical response of bacteria for (a) noninfected *E. coli* and (b) *E. coli* infected with M13 phages. The differences between the initial contact and final detachment point, which are defined as Δn, are shown in (c) and (d), respectively.

this work via the use of AFM imaging in liquid can be combined with the $f-d$ curve to provide an approach for investigating the relationship between cell fragility and membrane alteration after filamentous phage infection. This shows great promising for future studies, such as the time-dependent change in the bacterium−phage interaction.

Acknowledgment. This work was supported by the National Science Council under project no. NSC 96-2120-M-009-003. We also thank the CNMM, Professor F. G. Tseng and Professor W. K. Hsu at National Tsing-Hua University, and Professor L. Hsu at Chiao-Tung University for facility support on liquid AFM, contact angle measurements, and Young's modulus calculation, respectively.